

189  
84-125  
3/1-78

DA. 1875

UCRL-52388

# EXPLORATORY EXPERIMENTS COMPARING DAMAGE EFFECTS OF HIGH-ENERGY NEUTRONS AND FISSION-REACTOR NEUTRONS IN METALS

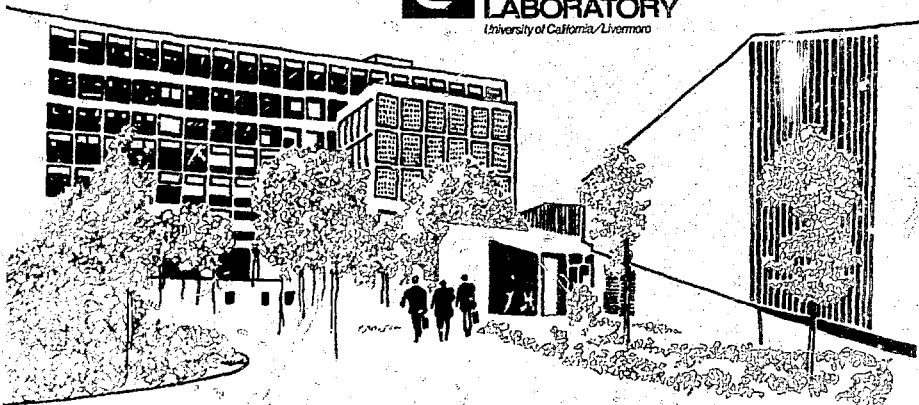
Jack B. Mitchell

January 12, 1978

MASTER

Prepared for U. S. Energy Research & Development  
Administration under contract No. W-7405-Eng-48

 **LAWRENCE  
LIVERMORE  
LABORATORY**  
*University of California/Livermore*





**LAWRENCE LIVERMORE LABORATORY**  
*University of California, Livermore, California, 94550*

UCRL-52388

**EXPLORATORY EXPERIMENTS  
COMPARING DAMAGE EFFECTS OF  
HIGH-ENERGY NEUTRONS AND  
FISSION-REACTOR NEUTRONS IN METALS**

**Jack B. Mitchell**

**MS. date: January 12, 1978**

**NOTICE**

This report was prepared as an account of work sponsored by the United States Government. Neither the United States nor the United States Department of Energy, nor any of their employees, nor any of their contractors, subcontractors, or their employees, makes any warranty, express or implied, or assumes any legal liability or responsibility for the accuracy, completeness or usefulness of any information, apparatus, product or process disclosed, or represents that its use would not infringe privately owned rights.

## CONTENTS

Abstract	1
Introduction	1
High-Energy Neutron Sources	2
Rotating-Target Neutron Source (RTNS)	2
Be(D,n) and Li(D,n) Stripping Sources	2
Experimental Procedure	4
Results and Discussion	5
References	10

# EXPLORATORY EXPERIMENTS COMPARING DAMAGE EFFECTS OF HIGH-ENERGY NEUTRONS AND FISSION-REACTOR NEUTRONS IN METALS

## ABSTRACT

Until the Rotating-Target Neutron Source II (RTNS II) and the Li(D,n) stripping source for high fluxes of high-energy neutrons are in operation, work related to DMFE's fusion-reactor materials and radiation-effects program is being conducted with lower-flux prototypes, the RTNS I at LLL and a Be(D,n) stripping source at the University of California, Davis. This paper describes these sources and presents results of some exploratory experiments in which 0.5-mm-thick tensile specimens of copper, vanadium, niobium, and Nb-1 wt% Zr alloy were irradiated by high-energy neutrons from these sources and by lower-energy neutrons from the Livermore Pool-Type Reactor (LPTR). After being irradiated, the specimens were tensile-tested, and the increases in their 0.2%-offset yield strengths were related to the neutron fluences and energies to which they had been subjected. In the pure metals, about 20 times as great a fluence of neutrons ( $E > 0.5$  eV) from the LPTR was required to produce the same increase in yield strength as RTNS 14-MeV neutron fluences above  $10^{17}$  n/cm<sup>2</sup>; the corresponding ratio for Be(D,n) neutrons to RTNS neutrons was about 1.3. To produce equal radiation strengthening in Nb-1 wt% Zr, the ratio of LPTR ( $E > 0.5$  eV) fluence to RTNS 14-MeV fluence was about 11; the enhanced strengthening of the alloy by lower-energy neutrons is perhaps attributable to higher substitutional impurities in the alloy. Presented in terms of yield-strength increase versus displacement damage energy (eV/atom), the results showed that the radiation strengthening in the pure metals was essentially identical for the RTNS and Be(D,n) sources, while it took about twice as much damage energy to produce the same strengthening with LPTR neutrons. Transmission electromicroscopy of the damage structures revealed that although the high-energy and lower-energy neutron irradiations produced the same kind of structural defects, the number densities and size distributions of the defects differed. Apparently, the fraction of radiation-produced damage retained in the form of point-defect clusters is greater for high-energy neutrons than for lower-energy neutrons primarily because of the increased recombination of the diffusing vacancies and interstitials during low-energy irradiation. In Nb-1 wt% Zr alloy, however, radiation strengthening versus damage energy was the same for RTNS and LPTR neutrons; this equivalence apparently results from trapping of point defects by the higher level of impurities in the material tested.

## INTRODUCTION

One of the major technological requirements for the successful operation of DT fusion power reactors is the development of materials for the first wall and related components that will retain their structural integrity in the radiation environment of high-energy (~14 MeV) fusion neutrons.

At the present time, little is known about the bulk radiation damage effects of high-energy neutrons on

the behavior of candidate materials for fusion reactors. We know that fusion neutrons will create a larger number of atom displacements per primary collision than lower energy (1-2 MeV) fast fission neutrons and that internal helium generation from (n, $\alpha$ ) reactions will be substantially greater for fusion neutrons than for fast fission neutrons. Thus, we expect that the deleterious effects of radiation

damage that have been experienced in fission-reactor materials will be even more severe in fusion reactors.

In order to satisfy the long-term materials performance requirements for commercial fusion power, the Division of Magnetic Fusion Energy, DOE, has instituted a materials and radiation effects program, one of whose primary objectives is to develop materials and an understanding of materials behavior that will assure the structural integrity of the first wall and related components. This program will utilize and correlate radiation effects data from fission reactors, ion irradiations, and high-energy neutron sources.

The high-energy neutron sources planned for this radiation effects program are the Rotating Target Neutron Source (RTNS II) currently under construction at the Lawrence Livermore Laboratory and an  $\text{Li}(\text{D},\text{n})$  stripping source which is in the design stage. These sources are expected to provide a neutron flux of  $10^{13}$  to  $10^{15}$  n/cm<sup>2</sup>-s.

At the present time there are lower-flux prototypes of these sources in operation: RTNS I at

LLL, and  $\text{Be}(\text{D},\text{n})$  stripping sources, one of which is at the University of California at Davis. Although radiation damage experiments on these lower-flux prototype sources are not generally useful for assuring the structural integrity of materials for the first wall of a fusion reactor in high neutron fluences ( $>10^{20}$  n/cm<sup>2</sup>), they can provide a basic understanding of the nature and magnitude of the damage effects of high-energy neutrons. Damage due to high-energy neutrons can be directly compared and correlated with damage due to ions and fission-reactor neutrons in order to assess any differences in the nature, quantities, and distributions of the damage and associated properties, and to provide a basis for increased confidence in simulation techniques with other sources of radiation.

This paper will describe the characteristics of the RTNS I and  $\text{Be}(\text{D},\text{n})$  high-energy-neutron sources and the results of some exploratory experiments using these sources to compare the nature and magnitude of the damage effects of high-energy neutrons and fission-reactor neutrons.

## HIGH-ENERGY-NEUTRON SOURCES

### Rotating-Target Neutron Source (RTNS)

The RTNS I has been described in detail elsewhere.<sup>1-5</sup> Essentially it consists of an insulated-core-transformer accelerator which produces a 400-keV deuteron beam that is focused onto a water-cooled target that rotates at 1100 rpm. The target is composed of a 9-in.-diameter Amzirc disk onto which a thin layer of titanium has been deposited and reacted with tritium to form titanium tritide. DT reactions take place in the target, and fusion neutrons are emitted with energies between about 14.1 and 15.6 MeV. The presently operating source (RTNS I) supplies a deuteron current of about 15 mA on target. The neutron source strength is  $5 \times 10^{12}$  n/s. The upgraded RTNS II will eventually supply a deuteron current of 400 mA on a larger target that rotates at 10,000 rpm. This source is expected to have a neutron source strength of  $\sim 10^{14}$  n/s and a maximum flux of about  $5 \times 10^{13}$  n/cm<sup>2</sup>-s.

### $\text{Be}(\text{D},\text{n})$ and $\text{Li}(\text{D},\text{n})$ Stripping Sources

The  $\text{Be}(\text{D},\text{n})$  stripping source at the Davis

campus of the University of California consists of a 76-in. isochronous cyclotron which produces a beam of 30-MeV deuterons that is focused onto a beryllium target. The target is of a thickness to completely stop a 30-MeV deuteron and is brazed onto a copper backing plate having channels for water coolant. High-energy neutrons are produced as a result of beryllium atoms in the target stripping away protons from the deuterons. The neutrons have a strongly forward-peaked flux and a broad energy spectrum that is peaked at about one half the deuteron energy. In addition to these high-energy neutrons from the deuteron stripping, a more isotropic flux of lower-energy neutrons is produced from compound nucleus reactions. The resultant differential neutron spectrum close to the beryllium target is shown along with the spectra for the RTNS and a fission reactor (LPTR) in Fig. 1. The spectrum and flux of neutrons from the stripping source will depend on position relative to the target as well as the deuteron energy.<sup>6</sup>

The Davis  $\text{Be}(\text{D},\text{n})$  source uses a 35- $\mu\text{A}$ , 30-MeV deuteron beam which produces a maximum neutron flux of  $7 \times 10^{12}$  n/cm<sup>2</sup>-s ( $E > 1.0$  MeV). The planned  $\text{Li}(\text{D},\text{n})$  source operates on the same principles as the  $\text{Be}(\text{D},\text{n})$  sources, but the target will

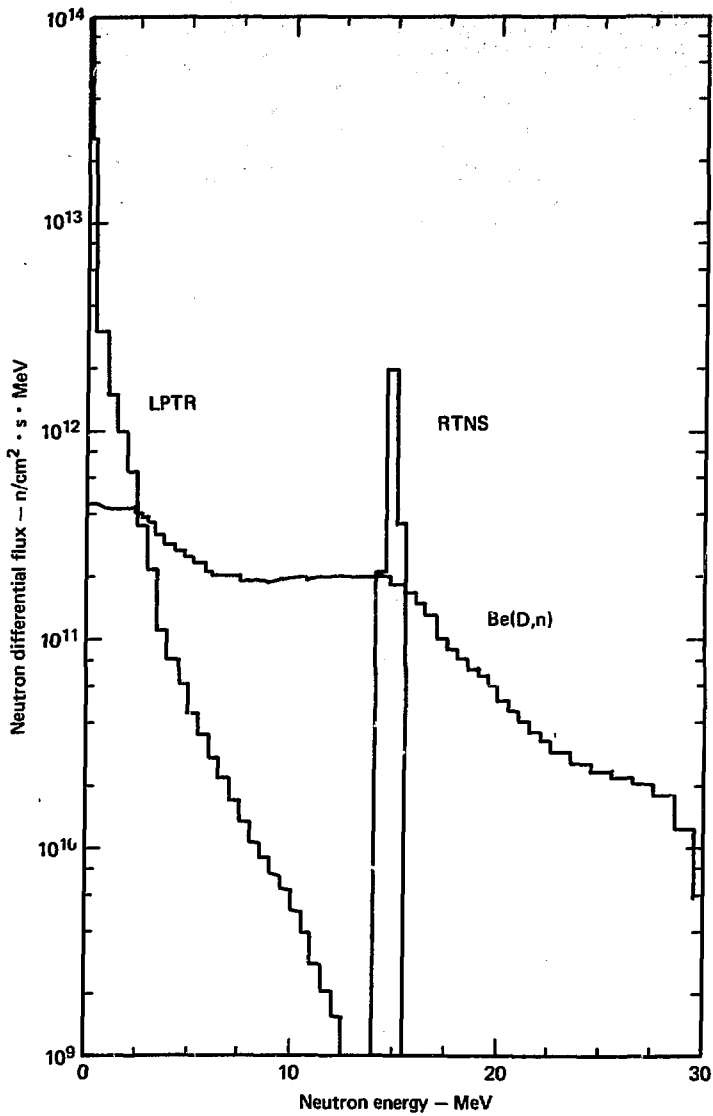


Fig. 1. Differential neutron spectra for the RTNS, Be(D,n), and LPTR sources.

be a rectangular jet of liquid lithium. High-energy (30–40 MeV) deuterons will be provided by a linear accelerator capable of delivering 100 mV on the

lithium target. The maximum neutron flux expected from the  $\text{Li}(D,n)$  source is approximately  $10^{15}$   $\text{n}/\text{cm}^2\text{-s}$  ( $E > 1$  MeV).

## EXPERIMENTAL PROCEDURE

Small tensile specimens of copper, niobium, vanadium, and Nb-1 wt% Zr, of the dimensions shown in Fig. 2, were machined from 0.5-mm-thick (0.020 in.) sheet stock. The chemical analysis of these materials is shown in Tables 1 and 2. The niobium and vanadium specimens were annealed for 1 hour at 1200 and 1000°C, respectively, in 0.13  $\mu\text{Pa}$  ( $\sim 10^{-9}$  torr) vacuum. The copper specimens were annealed for 1 hour at 600°C in 1.3 mPa ( $10^{-5}$  torr) vacuum, and the Nb-1 wt% Zr specimens were annealed for 1 hour at 1550°C in 0.13  $\mu\text{Pa}$  ( $10^{-9}$  torr) vacuum. These times and temperatures were selected to obtain grain sizes that would give at least ten grains over the 0.5-mm specimen thickness to insure reproducible polycrystalline tensile behavior.

Table 1. Chemical analysis of impurity elements in Cominco copper.

Element	Concentration (ppm)
Fe	400
Si	150
Mg	10
Ag	2
Ca	2
Co	<10
Ni	<3
Al	<3
Be	<1

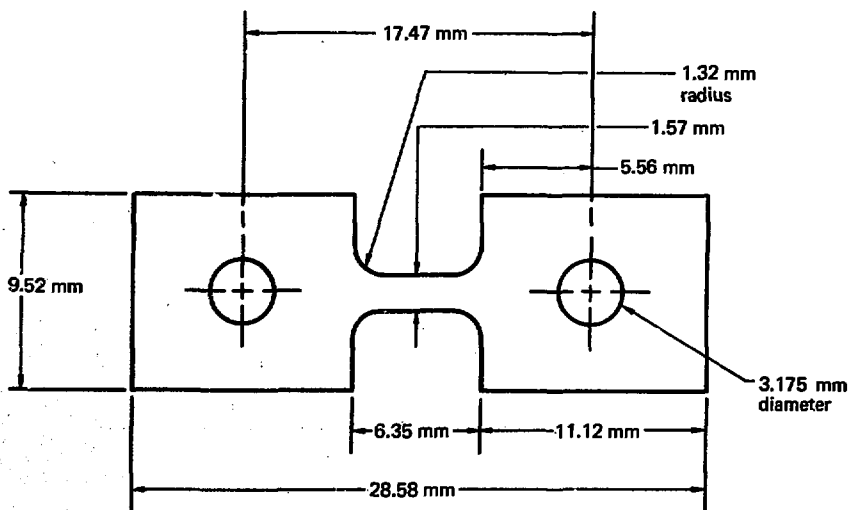


Fig. 2. Dimensions of irradiated tensile specimens.

Table 2. Chemical analysis of interstitial impurities in niobium, Nb-1 wt% Zr, and vanadium.

Element	Concentration (ppm)			
	LLL niobium	MRC <sup>a</sup> niobium	Nb-1 wt% Zr	MRC <sup>a</sup> vanadium
C	15	15	92	210
O	208	40	185	110
N	70	5	40	60

<sup>a</sup>Materials Research Corp.

Specimens were irradiated with the various sources as indicated in Table 3. Dosimeter foils were cut to the same shape as the tensile specimens and interspersed with them in stacks, so that each specimen in a stack was sandwiched between two foils.

For the ambient-temperature (25°C) irradiations on the RTNS and the Be(D,n) source, the specimens were stacked along with dosimeter foils in small epoxy-fiberglass laminated holders and placed as close as possible to the neutron source spot.

For elevated-temperature (210°C) RTNS irradiations, the tensile specimens were enclosed along with dosimeter foils in a platinum capsule and heated by a spot lamp heater.

For irradiation in the LPTR, the specimens along with dosimeter foils were enclosed in cadmium-lined aluminum cans. For the 65°C irradiations, the specimens were lightly pressed against a semicircular aluminum block that had good thermal contact with the inside of the can, and the heat transfer to the reactor cooling water, maintained at 40°C,

provided an ambient specimen temperature of 65°C. The 210°C LPTR irradiation temperature was obtained by gamma-ray heating by inserting the specimens with little contact with the inside of the can.

Dosimetry for the RTNS irradiations was accomplished by neutron activation and gamma-ray-counting niobium dosimeter foils for the reaction <sup>93</sup>Nb(n,2n)<sup>92</sup>Nb. The fluence value for each specimen was taken as the mean of the fluences calculated for the dosimeter foils in front and back of it. The absolute accuracy of the mean fluences is 7.5%.

Dosimetry for the Be(D,n) irradiations was accomplished by gamma-ray-counting iron dosimeter foils stacked with the tensile specimens. The dosimeter foil fluences were calculated by using spectrum-average cross sections for the reaction <sup>54</sup>Fe(n,p)<sup>54</sup>Mn. The absolute fluence value for each specimen was taken as the mean of the values calculated for the iron foils in front and back of it.

Fluence values for the LPTR irradiations were obtained from the spectrum-integral cross sections of iron dosimeter foils for the reaction <sup>54</sup>Fe(n,p)<sup>54</sup>Mn. The fluences determined in this way have an estimated uncertainty of ±15% for >1 MeV and ±30% for <1 MeV.

After irradiation and dosimetry measurement, the specimens were mounted in tensile grips in a specially designed jig to insure against deformation during handling and were tested in an Instron testing machine at about 26°C and a crosshead rate of 0.05 mm/min (0.002 in./min). The 0.2% offset yield stress was determined using the Instron crosshead motion as the sample extension.

Table 3. Materials, sources, and irradiation temperatures.

Material	Irradiation temperature (°C)		
	RTNS 1	Be(D,n)	LPTR
Copper	25; 210	25	65; 210
Vanadium	25	25	65
Niobium	25; 700	25	65
Nb-1 wt% Zr	25; 600	-	65

## RESULTS AND DISCUSSION

The increase in 0.2%-offset yield stress versus neutron fluence for tensile specimens of Cu, Nb, V, and Nb-1 wt% Zr are shown in Figs. 3, 4, 5, and 6, respectively. It is apparent from these plots that the

high-energy neutrons from the RTNS and Be(D,n) sources are considerably more effective than the lower-energy neutrons from the LPTR in strengthening all of the metals.

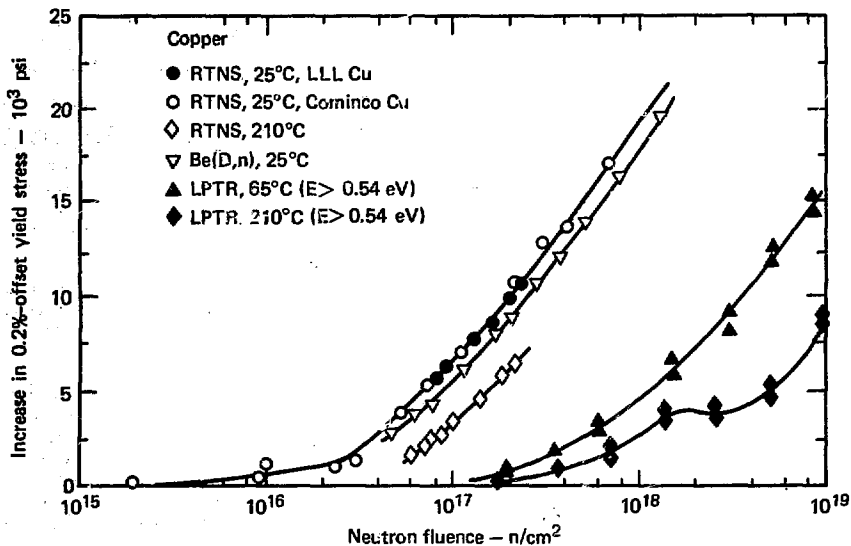


Fig. 3. Increase in 0.2%-offset yield stress vs neutron fluence for RTNS, Be(D,n), and LPTR irradiations of copper.

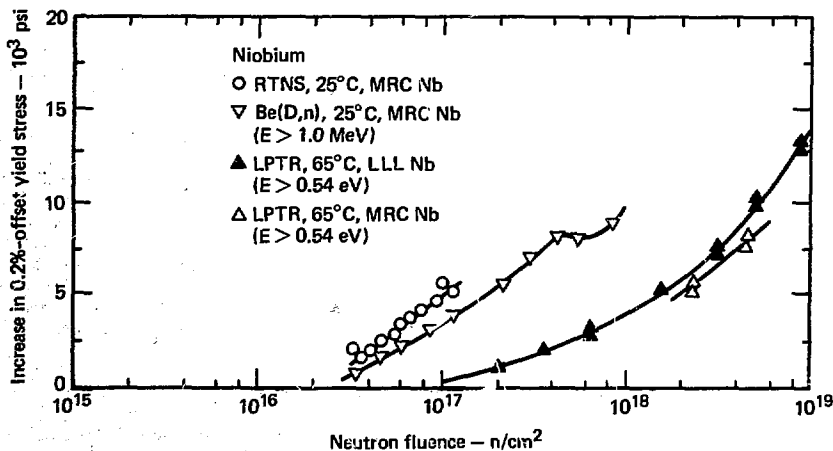


Fig. 4. Increase in 0.2%-offset yield stress vs neutron fluence for RTNS, Be(D,n), and LPTR irradiations of niobium.

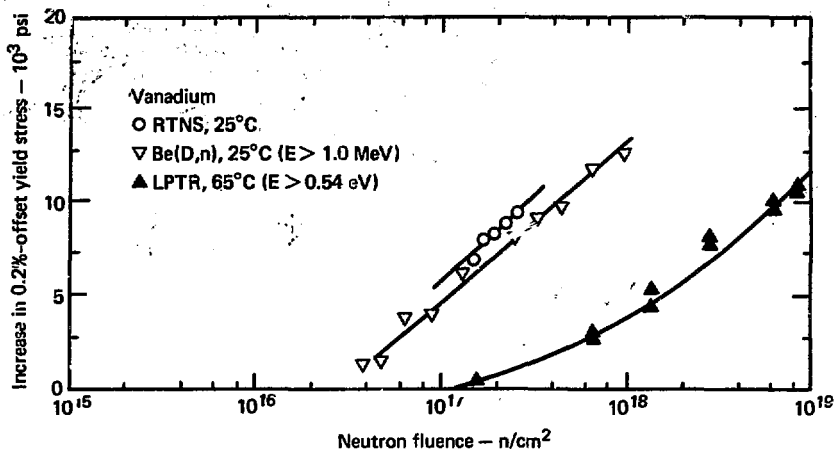


Fig. 5. Increase in 0.2%-offset yield stress vs neutron fluence for RTNS, Be(D,n), and LPTR irradiations of vanadium.

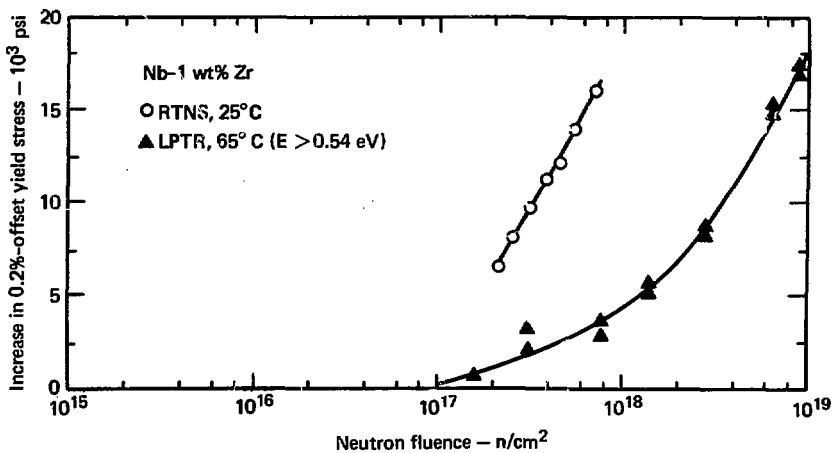


Fig. 6. Increase in 0.2%-offset yield stress vs neutron fluence for RTNS and LPTR irradiations of Nb-1 wt% Zr.

If we compare the 25°C RTNS and 65°C LPTR data for the Cu, Nb, and V, we find that about 20 times as great a fluence of neutrons ( $E > 0.5$  eV) from the LPTR is required to produce the same increase in yield strength as 14-MeV neutron fluences above about  $10^{17}$  n/cm<sup>2</sup>. (If the LPTR neutron fluence is expressed in terms of  $E > 0.1$  MeV, this ratio reduces to about 10.)

Comparison of the 25°C RTNS and Be(D,n) data gives a ratio of Be(D,n) neutrons ( $E > 1.0$  MeV) to RTNS neutrons of about 1.3 for the same strengthening.

LPTR irradiation produced greater strengthening in LLL Nb than in Materials Research Corp. (MRC) Nb. The only apparent difference between the two materials is the higher interstitial impurity content in the LLL Nb (see Table 2). It has previously been shown that interstitial impurities can significantly increase the radiation strengthening of Nb irradiated with fission-reactor neutrons.<sup>7</sup>

LPTR irradiation also produced greater strengthening in Nb-1 wt% Zr alloy than in Nb. In this case, however, the interstitial impurity content in the Nb-1 wt% Zr is only slightly greater than in

the LLL Nb (Table 2), and much of it should be combined with the Zr solute. Thus the greater radiation strengthening of the alloy can only be conjectured to be associated with its higher substitutional impurity content.

The 25°C RTNS results for Nb-1 wt% Zr and MRC Nb cannot be directly compared because the data are in different fluence ranges.

The ratio of neutron fluences from the LPTR ( $E > 0.5$  eV) and RTNS to produce the same increase in yield strength in Nb-1 wt% Zr is about 11 (or about 5.5 when counting LPTR neutrons above  $E > 0.1$  MeV). This ratio is about half that for the Nb, V, and Cu. It appears that this reduced ratio can be accounted for solely by the greater radiation strengthening produced by the LPTR in the Nb-1 wt% Zr.

RTNS irradiations of Nb at 760°C and fluences up to about  $10^{17}$  n/cm<sup>2</sup>, and of Nb-1 wt% Zr at 600°C and  $2.5 \times 10^{17}$  n/cm<sup>2</sup>, produced no observable radiation strengthening. At these elevated temperatures, apparently, annealing of the displacement damage moves the threshold for observable strengthening to a significantly higher fluence.

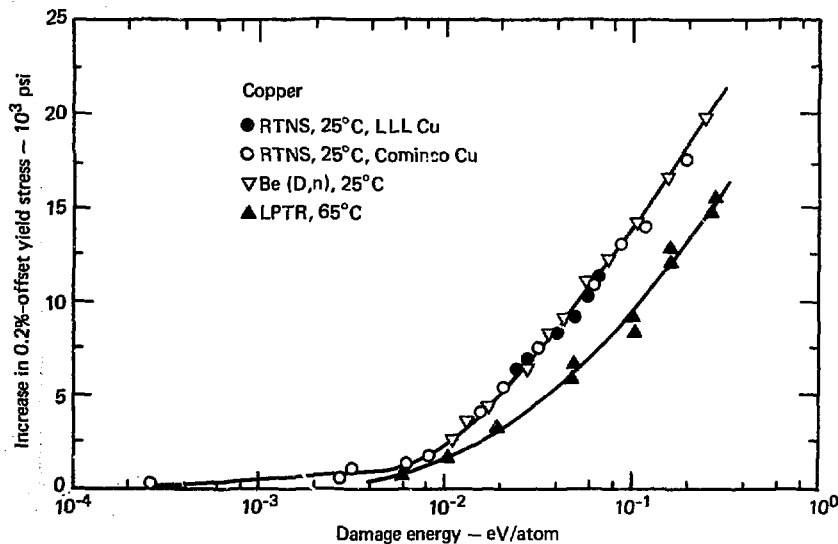


Fig. 7. Increase in 0.2%-offset yield stress vs damage energy for neutron-irradiated copper.

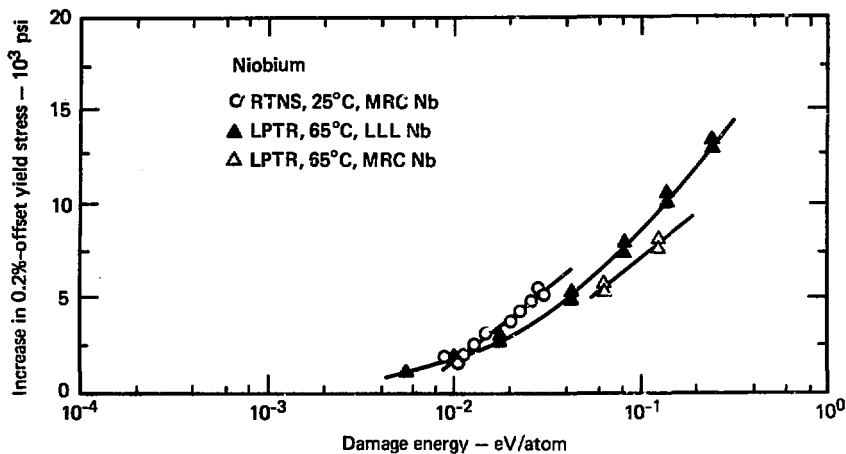


Fig. 8. Increase in 0.2%-offset yield stress vs damage energy for neutron-irradiated niobium.

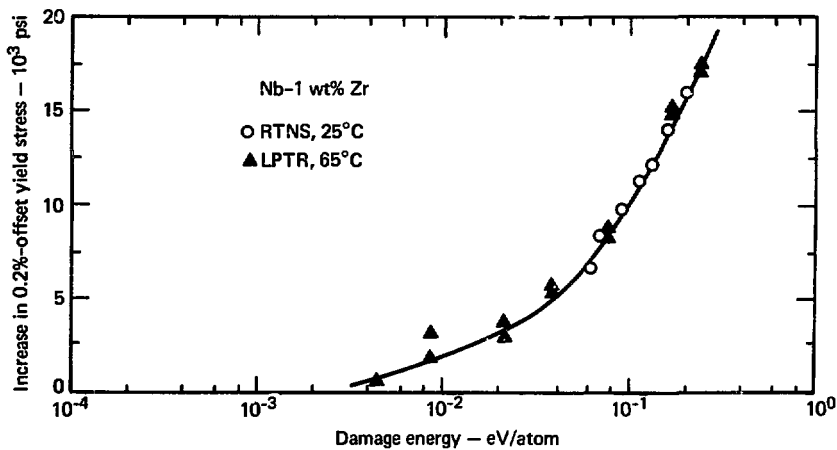


Fig. 9. Increase in 0.2%-offset yield stress vs damage energy for neutron-irradiated Nb-1 wt% Zr.

The ambient-temperature results for Cu, Nb, and Nb-1 wt% Zr in Figs. 3, 4, and 6 are replotted in Figs. 7, 8, and 9 as yield-strength increase versus displacement damage energy. These plots normalize the results with respect to the differences in neutron energies from the three sources.

Figures 7 and 8 show that the ambient-temperature radiation strengthening produced in Cu and Nb by RTNS and Be(D,n) irradiations are essentially identical on the basis of damage energy, whereas it takes about twice as much damage energy to produce the same strengthening with LPTR neutrons. The same effect would probably be observed in V.

These differences in radiation strengthening produced for the same amount of displacement damage energy result from differences in the resultant structural damage. Transmission electron-microscopy observations reveal that the damage structures produced by the RTNS, Be(D,n), and LPTR irradiation consist of the same kind of primary defects, i.e., vacancy and interstitial clusters and small frank and prismatic dislocation loops.<sup>8</sup> In the pure metals irradiated to a given damage energy level, the damage structures produced with high-energy RTNS and Be(D,n) neutrons appear to differ from those produced with lower-energy LPTR neutrons in the number density and size distribution of the defects. These structural differences appear to arise from the differences in neutron energy as follows.

During irradiation with the high-energy neutrons, most of the damage energy (~85%) is produced in displacement cascades with energies greater than 100 keV. These high-energy cascades spontaneously create stable vacancy clusters from the vacancies in the cascade. The self-interstitials form clusters by coalescence.

By contrast, during irradiation with the neutron spectrum from a fission reactor, most of the damage energy (~80%) is produced in lower-energy cascades, <50 keV. Unlike the high-energy cascades, these do not spontaneously form vacancy clusters. The majority of the clusters are formed by diffusion-controlled coalescence of interstitials and vacancies.

That the fraction of radiation-produced displacement damage retained in the form of point-defect clusters is greater for high-energy neutrons than for fission-reactor neutrons appears to be primarily because of the increased recombination of the diffusing vacancies and interstitials during irradiation with fission-reactor neutrons.

For Nb-1 wt% Zr, Fig. 9 shows that the yield-strength increase produced by the RTNS and LPTR neutrons scales with damage energy. This result is different from that for the pure metals; as previously discussed it appears to arise from the greater radiation strengthening of Nb-1 wt% Zr relative to Nb during the LPTR irradiation. It appears that the enhanced radiation strengthening of Nb-1 wt% Zr results from trapping of the point defects by the higher content of impurities.

## REFERENCES

1. R. Booth, *IEEE Trans. Nucl. Sci.* NS14, 943 (1967).
2. R. Booth and H. H. Barschall, *Nucl. Instrum. Methods* 99, 1 (1972).
3. R. Booth, H. H. Barschall, and E. Goldberg, *IEEE Trans. Nucl. Sci.* NS20, 472 (1973).
4. R. Booth, *Nucl. Instrum. Methods* 120, 353 (1974).
5. R. A. Van Konynenburg, H. H. Barschall, R. Booth, and C. Wong, *Proc. Intl. Conf. Radiation Test Facilities for the CTR Surface and Materials Program*, Argonne National Laboratory, July 15-18, 1975.
6. D. R. Nethaway, R. A. Van Konynenburg, M. W. Guinan, and L. R. Greenwood, *Proc. Symposium on Neutron Cross Sections, 10-40 MeV*, Brookhaven National Laboratory, May 3-5, 1977 (also Lawrence Livermore Laboratory report UCRL-79557).
7. B. A. Loomis and S. B. Gerber, *Acta Met.* 21, 165 (1973).
8. J. B. Mitchell, R. A. Van Konynenburg, C. J. Echer, and D. M. Parkin, *Intl. Conf. Radiation Effects and Tritium Technology for Fusion Reactors*, Gatlinburg, Tennessee, Oct. 1-3, 1975.